AD A118262

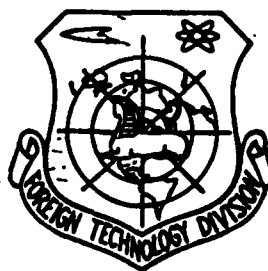# FOREIGN TECHNOLOGY DIVISION

TRANSONIC TEST ON THE BALLISTIC RANGE

by

Zheng Zhichu, Wang Xigi, et al.

AUG 1 7 1982

82 08 16 124

EDITED TRANSLATION

GRAPHICS DISCLAIMER

All figures, graphics, tables, equations, etc.
merged into this translation were extracted
from the best quality copy available.

TRANSONIC TEST ON THE BALLISTIC RANGE[*]

Zheng Zhichu, Wang Xigi, Wang Jiurui, Li Binglu, Hau Zhong, Zhang
Zhensong, Ge Xuezheu, Zeng Jianguo, Zhang Zhengxin, Ma Wenju,
Jia Yufang
(Institute of Mechanics, Academia Sinica)

ABSTRACT

This paper introduced new methods of transonic ex-
periments using ballistic range. Two new special tech-
niques have been used on a two-stage light gas gun--
namely, the filing gas launching technique which can be
used to reach a subsonic projectile velocity range and
the low filling condition which can launch projectiles
to reach transonic and supersonic velocity regions.
Because the initial acceleration is smaller, the models
launched have an undamaged configuration and stable atti-
tude. In addition, there is no support disturbance and
small wall effect which makes the ballistic range facil-
ity more superior in transonic experiments. Using the
forementioned techniques, clear photographs of flow
field around spheres in transonic cases have been obtained.
Compared with supersonic and hypersonic flows, the stand-
off distance of a shock wave, the position of the separa-
tion point, the neck width and the wake are apparently
quite different. In this paper, two photographs of the
entire flow field at $M = 1.01$ and $M = 0.99$ are very
meaningful. Finally, an idea to raise the Reynolds num-
ber up to 10^7 by increasing the pressure and decreasing
the temperature in the ballistic range is described.

I. INTRODUCTION

Since the transonic throat passage in a Laffar shock tube, the
study of transonic flow has been in existence for nearly 100 years.
However, due to the difficulties involved in mathematics and exper-
imental tools, the progress in this particular field was very slow
before the 40's in this century.

After the 40's, in order to solve the "sonic barrier" problem,

the study of transonic flow became more important. In 1945, the
open groove wall was born. Subsequently, the multi-hole wall
appeared in order to eliminate the plugging phenomenon and thus
established the basic condition of transonic wind tunnels. It
opened the avenues for research and development in this field. In
the late 50's, the dynamic revolution made aircraft break-through
the sonic barrier to reach hypersonic speeds. In order to pursue
the insights in this area, many scientists were attracted to this
field; thus the study of transonic flow suffered the so-called
"hypersonic" crisis [1].

In recent years, the development of computers has been advanta-
geous to the numerical analysis of transonic flow. The discovery
of new wings which have good aerodynamic characteristics at tran-
sonic speed has received a lot of attention in the aerodynamic
societies across the world. Therefore, the study of transonic flow
once again became active. The two peaks of the wave shown in Figure
1 [2] reflect the two active periods of transonic flow studies. The
latter peak seemed to indicate a new direction in aerodynamic research.

Figure 1. The development
of transonic studies
1--reports; 2--year
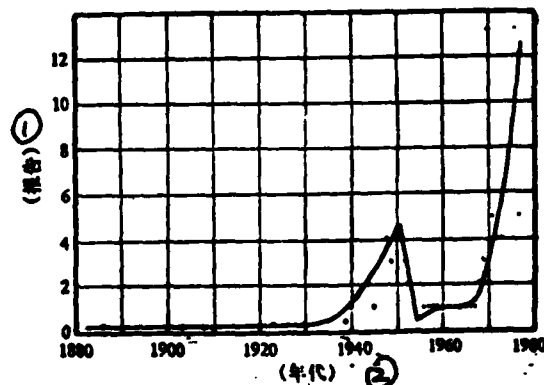
At the present moment, the importance of research on transonic
flow at high Re numbers was brought about due to the need to increase
the speed and enlarge the size of transport aircrafts. The "C-141"
incident indicated that the low Reynolds number in the wind tunnel
would create serious problems. The differences in shock wave posi-
tion, separation point and aerodynamic force distribution at low Re
numbers and high Re numbers have caused great losses. It promoted
interest in the experimental equipment for transonic studies at

2

high Re numbers. At the present moment, the United States has invested over 100 million dollars in this area. The wind tunnel work group of NATO is also preparing a high Re number transonic experiment facility for common use. Besides the construction of larger dimension transonic wind tunnels, quite a few special devices have been invented, such as refrigerated wind tunnel, Ludwitch tube, Evans tube and even shock tubes were included in the transonic experiments [3-6].

This paper introduces two new launching techniques which enable a two-stage light gas gun to launch models to reach subsonic and transonic speeds. On top of that, there is no support disturbance on the model, no small wall effect and one can economically vary the Re number. These advantages demonstrated the unique capabilities of this ballistic range apparatus in the many aspects of transonic studies, such as the display of flow field, the lengthening of the wake, resistance coefficient, separation flow and stability. It has become an important tool.

II. LAUNCHING TECHNIQUES

In [7], the ballistic range was described as a simulation test apparatus which is capable of doing anything within the range between M 1~30 as shown in Figure 2. In the transonic and supersonic speed region, regular guns are usually used as the launching device both domestically and abroad. If it is possible to use a light gas gun to simultaneously realize subsonic, transonic, supersonic and hypersonic velocities, then it is a new means to make this device become a multi-functional apparatus. It is a connector to link the classical aerodynamic trajectory target and the new super high special ballistic range.

Subsonic launching using a light gas gun can be accomplished without loading charges, and a direct gas fill method can be used. The principle is shown in Figure 3a. The compression tube is used as a gas storage tube. The model is isolated by a diaphragm. The

3

maximum pressure of the gas storage tube and the release pressure of the model are both controlled by the diaphragm. When the compression tube pressure rises to a certain value, the diaphragm breaks and the gas launches the model. Let us assume:

1. The driving gas flows into the launching tube at sonic speed,
2. For low velocity launching, the frictional force of the model during launching can be estimated by the minimum pressure P_f of the minimal starting model. Using the equation of motion

$$m_s \frac{du}{dt} = (P_s - P_f)A_s \tag{1}$$

and the base pressure equation:

$$P_s = P_0/E\left(1 \mp \frac{A_s X}{V_0}\right)^{-\gamma} \tag{2}$$

Based on the assumptions and substituting equation (2) into (1) and integrating the equation, the exit velocity of the model is

$$u_s = \left[\frac{2P_0 V_0}{(\gamma - 1)m_s} \cdot \frac{(1 - B)}{E} - \frac{2P_f A_s l_s}{m_s}\right]^{\frac{1}{2}} \tag{3}$$

where
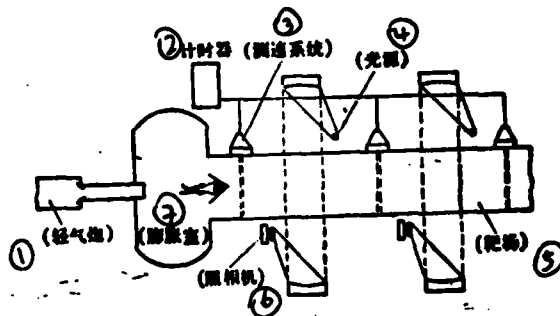
Figure 2. Schematic diagram of the trajectory target apparatus.
1--(light gas gun); 2--timer; 3--(velocity measuring system);
4--(light source); 5--(range); 6--(camera); 7--expansion chamber

$$B = \left(1 + \frac{A_s l_s}{V_0}\right)^{-(\gamma-1)} \qquad E = \left[1 + \frac{1}{2}(\gamma - 1)\right]^{\frac{\gamma}{\gamma-1}}$$

V_0 is the effective volume of the compression tube, l_s is the length of the launching tube, A_s is the cross-sectional area of the launching tube, P_0 is the gas pressure of compression tube, m_s is the mass

Figure 3(a). Schematic diagram
of low energy launching.
1--diaphragm; 2--piston (m_p);
3--gas fill port; 4--diaphragm;
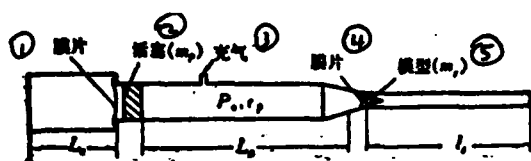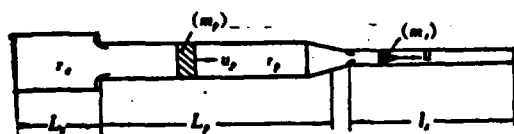5--model (m_s)

Figure 3(b). Schematic diagram
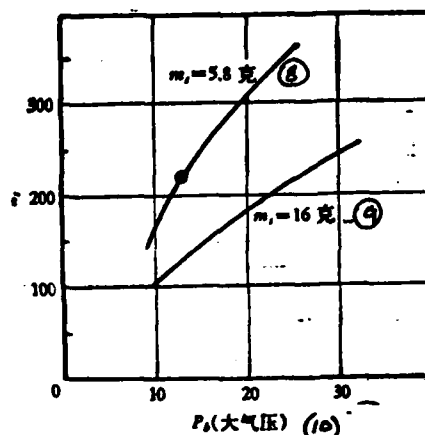of low energy transfer launch-
ing.

Figure 4. Curves showing the
relationship between model mass
and exit velocity ●本文实验 ⑫
8--m_s=5.8 g; 9--m_s=16 g; 10--P_b(atm)
12--experimental result in this
work

of the model and for Figure 7 the model $P_f \approx 2-3 \, \text{kg/cm}^2$. Using
this technique, subsonic launches were realized by a 13 mm diameter
light gas gun. Figure 4 shows the exit velocity vs. gas pressure
curves for two different model masses.

In the transonic velocity region, a low energy transfer launch-
ing method is used, which involves the use of low filling conditions
and a low pressure diaphragm-breaking technique to shatter the dia-
phragm not too long after the piston begins to move when the com-
pression tube pressure is not too high. The model moves under a base
pressure which is not too high even before the piston reaches the
high pressure chamber, or the piston has already stopped; or the
model has already exited. Therefore, the diaphragm breaking pressure
and the charge loading amount become important parameters in the
adjustment of velocity. Due to the fact that the base pressure is
slightly higher than in the subsonic case, for convenience in com-
putation, it is possible to neglect the frictional pressure P_f and
introduce an average pressure $\overline{P}_s$,

$$\overline{P}_s = \frac{1}{l_s} \int_0^{l_s} P_s \, dx$$

Using the above assumptions to improve the computation of equation (8), the exit speed u_s and $\overline{P}_s$ can be obtained by solving equations (4) and (5) simultaneously.

$$u_s = \left(\frac{2A_s l_s}{m_s}\,\overline{P}_s\right)^{\frac{1}{2}} \tag{4}$$

$$u_s = F(gRT_o/\overline{M})^{\frac{1}{2\gamma_p}} \cdot \left(\frac{\overline{P}_s}{m_s} \cdot V_o\right)^{\frac{\gamma_p-1}{2\gamma_p}} \tag{5}$$

where

$$F = \left(\frac{2\gamma_p}{\gamma_p - 1}\right)^{\frac{1}{2}} \cdot (\overline{P}_{max} - 1)^{\frac{-(\gamma_p-1)}{2\gamma_p}}\left[(\overline{P}_{max}^{\frac{\gamma_p-1}{\gamma_p}} - 1)^{\frac{1}{2}} + \left(\frac{2}{\gamma_p - 1}\right)^{\frac{1}{2}} \cdot (\overline{P}_{max}^{\frac{\gamma_p-1}{2\gamma_p}} - 1)\right]$$

$$\overline{P}_{max} = P_{max}/E\overline{P}_s$$

P_{max} is the maximum pressure in the high pressure chamber of the light gas gun. For a given launching-device with an initial gas filling pressure P_o, piston mass m_p and diaphragm breaking pressure P_b, P_{max} can be obtained from the following equation:

$$P_{max} = P_b \left[1 + \frac{(\gamma_p - 1)m_p u_{pb}^2}{2(L_p - x_i)P_b A_p}\right]^{\frac{\gamma_p}{\gamma_p-1}} \tag{6}$$

$$P_b = P_o \left[1 + \frac{1}{2}(\gamma_p - 1)M^2\right]^{\frac{\gamma_p}{\gamma_p-1}} \Big/ \left(1 - \frac{x_i}{L_p}\right)^{\gamma_p} \tag{7}$$

$$u_p^2 = \frac{2A_p P_{co} L_p \eta_1}{m_p}\left\{I + \frac{P_o\left[1 + \frac{1}{2}(\gamma_p - 1)M^2\right]^{\frac{\gamma_p}{\gamma_p-1}}}{P_{co}\eta(\gamma_p - 1)}\left[1 - \left(1 - \frac{x}{L_p}\right)^{1-\gamma_p}\right]\right\} \tag{8}$$

where

$$I = \frac{L_c}{L_p} \cdot \frac{1}{e(1 - \gamma_c)}\left[\left(1 + e\frac{x}{L_c}\right)^{1-\gamma_c} - 1\right]$$

The above expression provides the analytical expression of the relation between diaphragm breaking pressure and exit velocity which is not available in the usual light gas gun computation. Figure 5 shows the P_b and u_s relationship curves for two model masses. Figure 6 shows the relation between P_b and P_{max}. It can be seen from Figure 5 that: different charge loading will reach a different launching velocity. In addition, different from the hypersonic case, in the transonic case it is possible to use the sensitive region of the diaphragm breaking pressure with respect to exit velocity to control P_b
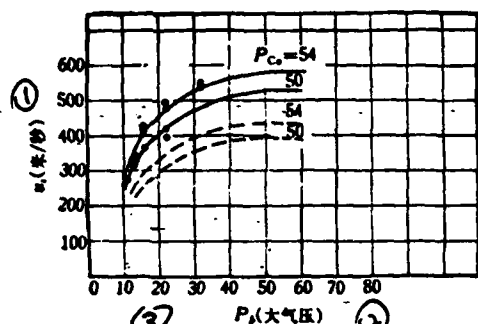
Figure 5. The relation between diaphragm breaking pressure and exit velocity
1--u_s(m/sec); 2--P_b(atm)
3---m_s=8g; 4--m_s=16 g. Experimental results of this work
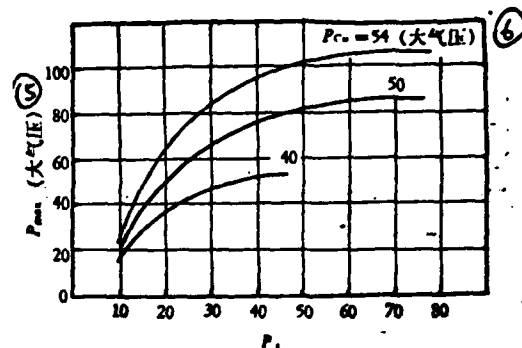
Figure 6. The relation between diaphragm breaking pressure and maximum pressure
5--P_{max}(atm); 6--P_{co}=54 (atm);

Figure 7. Schematic diagrams of the spherical model and its evolution body launched by a light gas gun.
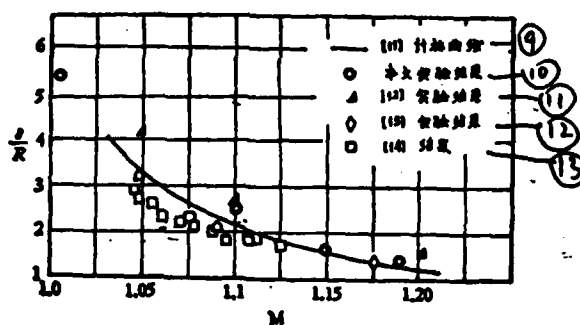
— [11]计算曲线 ○ 本文实验结果 ▲ [12]实验结果 ◇ [13]实验结果 □ [14]结果

Figure 8. Comparison of theoretical and experimental results of the stand-off distance of shock waves of a sphere.
9--calculated results in [11]; 10--experimental results of this work; 11--experimental results of [12]; 12--experimental results of [13]; 13--results of [14]; 15--calculated curves from [11]
o experimental results in this work ▲ experimental results in [12]
◇ experimental results in [13] □ results in [14]

7

in order to obtain the desired u_s. This is much more economical
and simpler than the complicated change of the tubes of a wind
tunnel and altering the experimental sections in order to realize
a varying M number.

III. FLOW FIELD OF SPHERE

The subsonic and transonic experiment in the small ballistic
range are the symbols of success of the above-mentioned launching
technique. Figure 7 gives the structure of the model. The photo-
graph 1 in the plate of Figure II shows the flow fields around the
sphere at various M numbers. In the experiment, paper diaphragm,
aluminum foil diaphragm, adhesive tape diaphragm and synthesized
diaphragm were used and the results proved that the control of velo-
city and the design of the model are successful.

In the results obtained, the two photographs of sphere flow at
$M \approx 1.010$ and $M \approx 0.990 (Re^* \approx 2.3 \times 10^5)$ are very significant. As is common-
ly known, at near $M \approx 1$ small variations in M number have a very
large effect on the flow field. Using the stand-off distance of
shock waves and the angle of incline of shock wave θ as examples,
if $M_\infty \gg 1, \delta \to 0, \theta \to 0$ but when $M \to 1$, $\delta \to \infty, \theta \to \frac{\pi}{2}$. The results in
this work showed that when $M \approx 1.010$ $\delta/R \approx 5.2, \theta \to \frac{\pi}{2}$ and when $M \approx 0.99$
the stand-off shock wave disappeared. These results have success-
fully proved this point. For various types of transonic equipment,
it is not possible to obtain the flow field at $M \approx 1$, because of
the serious congestion effect and wall hole disturbance at $M \to 1$.
The transonic experiment on the ballistic range can solve this prob-
lem very effectively. In addition, the photographs in the figures
also indicate that the effect of the M number becomes more signifi-
cant in the region $1 < M_\infty < 1.1$. Figure 8 shows the comparison between
the results obtained in this work and theory. In the region $M > 1.05$
the results obtained in this work are consistent with those in
[10], [11], [12] and [13]. At $M \approx 1$, this work provided data
points which are hard to obtain using other experimental devices.

The base flow of an aircraft has a significant effect on the aerodynamic force and aerodynamic heat. Under hypersonic and supersonic conditions, the base flow can be partially observed in the wind tunnel through the reduction of support cross-section and tension line techniques. In transonic conditions, especially near $M \approx 1$, the wall hole effect and support disturbance become so serious that it is very difficult to study the wake in the wind tunnel. The variation of the base flow characteristics at a transonic velocity, on the other hand, is intriguing enough to make researchers interested in obtaining the flow pattern. Here the ballistic range once again demonstrated its superiority. Comparing photograph 1 with photograph 2 in the plate figure in this paper, it shows that at transonic velocities: —

(1) the separation point of the flow moves forward

(2) the neck width diameter ratio increases, $d/D \approx 1$.

(3) at $M < 1$ the tail shock wave still exists, when $M < 0.95$ it disappears

(4) the wake increases and rapidly becomes irregularly shaped. It seems to have a large turbulent micro-circulating motion similar to a Carman whirlpool.

These results provided reliable basis to the study of the establishment, the separation flow and the wake of the transonic flow model.

IV. INCREASING Re NUMBER

The success in the ballistic range transonic experiment can be used as a basis for the study of the effect of the Re number. Many wind tunnel simulation experiments indicate that: The reliability of the data for $Re < 1 \times 10^6$ is very low, for $Re > 3 \times 10^6$ the data vary very smoothly, if $Re > 4 \times 10^7$ the Reynolds number has very little effect on the aerodynamic characteristics [4]. Therefore, the effect of the Reynolds number under transonic conditions is a very important problem. In general, there are three ways to increase the Reynolds number:

(1) to increase the dimensions of the model which means to enlarge the equipment

(2) to increase environmental pressure which means to increase density

(3) to decrease environmental temperature (increase density and decrease viscosity).

Using any one of the three means, it is possible to develop independent unique transonic apparatus such as the refrigerated wind tunnel, a regular transonic wind tunnel with large dimensions, Ludwitch tube, etc.

The methods mentioned above can all be realized for the ballistic range. Therefore, a simple small ballistic range can be used to carry out experimental studies on the effect of the Re number. In a small launching device capable of launching 10-15 mm diameter models, equipped with a 400 mm diameter, 5 m long range at normal temperature and pressure (based on the model shown in Figure 7 to carry out the experiment), the sphere has $Re^* \approx 2.7 \times 10^5$ and its revolved body $Re^* \approx 1.5 \times 10^6$. If the pressure of the target range is increased to 5 atm and the temperature is decreased to $T_{environment} \approx 73° K$, the combined effect can raise the Re* number to above 10^8 . Table 1 shows the Reynolds number under three different conditions. If the range is evacuated to 10^{-1} to 10^{-2} atm, Re* can be decreased to 10^3 . Since the volume of the range is small, pressurization, evacuation and refrigeration can be easily realized. With regard to the revolved body as shown in Figure 7 after lowering temperature and increasing pressure, there was no unstable effect caused by the rapid increase in flight resistance. Therefore, this experimental method has a very significant meaning in the observation of transonic separation flow, shock wave and adhesion layer interference and the effect of Re number on them.

TABLE 1. The Re numbers of two different bodies in flight under different environments

物 体 ②	特征长度 (毫米) ③	飞行速度 (米/秒) ④	环 境 条 件 ⑧		
			P = 1 (大气压) ⑤ T = 283°(K)	P = 8(大气压) ⑥ T = 283°(K)	P = 8(大气压) ⑦ T = 83°(K)
圆 球 ⑨	10	400	Re≈2.74 × 10⁵	Re≈2.19 × 10⁷	Re≈3.1 × 10⁷
旋成体 ⑩	55	400	Re≈1.51 × 10⁶	Re≈1.21 × 10⁷	Re≈1.72 × 10⁸

Key: 2--object; 3--characteristic length (mm)- 4--flying velocity (m/sec); 5--(atm); 6--(atm); 7--(atm); 8--environmental conditions; 9--sphere; 10--revolved body

V. CONCLUSIONS

1. The filling gas and low filling, low energy transfer techniques proposed in this paper are effective methods to solve the launching of subsonic, transonic and supersonic velocities for a two-stage light gas gun. Using various charge loading and diaphragm shuttering pressures, it is possible to effectively control the launching velocity.

2. During the transonic launching in the ballistic range, it is possible to simulate the full flow field more correctly because the diaphragm shuttering pressure is low, the initial overload of the model is small, the disturbance at the muzzle is little and the attitude of the model launched is stable.

3. The ballistic range can be evacuated, pressurized, cooled and varied in dimension so that the Reynolds number can be either raised or lowered. In the study of certain phenomena regarding the Re number, the trajectory range is economical, effective and easy to realize. Compared with the expensive transonic equipment currently under construction internationally, it has a persistent life.

4. The experimental results in the work, as compared with those obtained by wind tunnels or other apparatus, clearly indicated that the flow field varied significantly near $M^* \overset{\sim}{\sim} 1$ $(Re^* \approx 2.3 \times 10^5)$ Using sphere separation shock wave as an example, when $M_\infty \to 1$, δ/R

increases rapidly and the angle of incline for the shock wave $\theta \to \frac{\pi}{2}$. When M is slightly less than 1, a separation shock wave immediately disappears. When $M_\infty < 0.90$ $(Re^* \approx 2.3 \times 10^5)$ the shock wave near the wake also disappears.

5. The experiment of the wake demonstrated again that the ballistic range is superior over the wind tunnel. Unlike the supersonic condition, the separation point of the sphere tail flow field shifts forward, the neck width diameter ratio increases $d/D \approx 1$; the wake increases and quickly becomes irregular in shape with large turbulent micro-circulating motion.

REFERENCES

[1] 孙以钧, 国外航空简报, 1 (1974).
[2] 林同骥、贾振学, 中国科技大学专题讲义.
[3] 重见孝; 力学译丛, 4(1976).
[4] 俚起麟, 气动研究与发展, 3(1978).
[5] 徐永定, 气动力学刊, 1(1979).

[6] Cook, W. J., Presley, I. L., Chapman, G. T., AIAA paper 78—769.
[7] Solnoky, P., C. A. S. J., 15. 9(1969).
[8] Curtis, John, S., Third Hypervelocity Techniques Symposium (1964), 8.).
[9] Truying, Hsien, AIAA paper, 75—83.
[10] Van Dyke, M. D. & Gordon, H. D., NASA TR R-1 (1959).
[11] Heberle, J. W., Wood, G. P. & Gooderum, P. B., NACA TN 2000 (1950).
[12] Stilp, A., Bericht Nr. 10/65, Ernst-Mach-Institut, Freiburg, Br. Eckerstrasse 4, German (1965).